A&A manuscript no.
(will be inserted by hand later)

Your thesaurus codes are:
10 (10.15.2 NGC 2355; individual: 08:11.1; 08.18.1; 08.06.3)

ASTRONOMY AND ASTROPHYSICS
March 22, 2000

Fundamental properties of the open cluster NGC 2355

C. Soubiran, M. Odenkirchen, J.-F. Le Campion

Observatoire de Bordeaux, BP 89, F-33270 Floirac, France

Received ; accepted

Abstract. NGC 2355 is an old open cluster in the outer part of the galactic disk ($l = 203.^\circ4$, $b = +11.^\circ8$) which has been little studied until now. This paper presents the first astrometric and spectroscopic investigation of this cluster. We have measured precise absolute proper motions from old Carte du Ciel plates, POSS-I plates and recent CCD observations obtained with the Bordeaux meridian circle. The proper motion data reveal 38 highly probable cluster members down to $B_{\rm lim} = 15$ mag within $7'$ of the cluster center. We have also obtained ELODIE high resolution spectra for 24 stars. Seventeen of them are confirmed to be members of the cluster on the basis of radial velocity. Eight of them are fast rotating turnoff stars for which the projected rotational velocity has been determined. The spectroscopic observations have also provided estimates of the physical parameters $T_{\rm eff}, \log g$, [Fe/H], $M_{\rm V}$ of the 24 target stars. Two stragglers have been identified in the cluster. Combining our astrometric and spectroscopic results with previous UBV photometry and recent JHK$_s$ photometry from the 2MASS survey we have derived the fundamental properties of the cluster: metallicity, age, distance, size, spatial velocity and orbit.

Key words: Galaxy : open clusters and associations: individual: NGC 2355 – stars : kinematics – stars: rotation – stars: fundamental parameters

1. Introduction

Old open clusters, with ages greater than the age of the Hyades ($\sim$ 600 Myr), represent a minority of about 80 objects among 1200 known open clusters. Among their properties which enable to investigate both stellar physics and galactic structure (reviewed by Friel 1995), we are especially interested in orbits because they are related to the processes which have allowed them to survive tidal forces. The statistics are still poor but it seems that old open clusters follow orbits that keep them away from the plane and the disruptive effects of giant molecular clouds. The question is to know if these orbits result from special events or represent the tail of the distribution of clusters that have already been destroyed. Another relevant point to clarify is the relationship between orbits and metallicity [Fe/H] which traces the dynamical and chemical evolution of the Galaxy. The metallicity of old open clusters is intermediate between the disk and the thick disk, with a radial gradient, but a large dispersion that could indicate an inhomogeneous enrichment of the Galaxy. To answer such fundamental questions, new observations are needed to investigate in more details the old open cluster properties and their correlations. We have therefore undertaken a spectroscopic and astrometric program to obtain metallicities, distances and velocities of high quality for several poorly known old open clusters, NGC 2355 being our first target.

There are very few references on NGC 2355 in the astronomical literature. A photometric study in UBV down to $V \sim 19.2$ was made by Kaluzny & Mazur (1991). In this study, the reddening of the cluster was estimated to be E_{B-V}=0.12 mag, the distance modulus $(m-M)_0 = 12.1$, the metallicity +0.13 and the age the same as Praesepe. In their search for old open clusters, Phelps et al. (1994) also report a photometric study of NGC 2355 in BV but the photometry of individual stars is not given. Their calibration of the index δV, defined as the magnitude difference between the main-sequence turnoff and the giant clump leads to a Morphological Age Index corresponding to 0.9 Gyr, like Praesepe (Janes & Phelps 1994). More recently, Ann et al. (1999) examined this cluster as part of the BOAO survey (Bohyunsan Optical Astronomy Observatory, Korea) and determined from UBVI photometry : [Fe/H] $= -0.32, E_{B-V} = 0.25, (m-M)_0 = 11.4$ and an age of 1 Gyr.

⋆ based on observations made on the 193cm telescope at the Haute-Provence Observatory, France, and on plate digitisation at the Centre d'Analyse des Images, Paris. This publication makes use of data products from the Two Micron All Sky Survey, which is a joint project of the University of Massachusetts and the Infrared Processing and Analysis Center, funded by the National Aeronautics and Space Administration and the National Science Foundation.

Send offprint requests to: C. Soubiran

In Sect. 2 and 3 we present new data which are used to analyse the cluster in combination with the UBV photometry of Kaluzny & Mazur (1991) and the JHK$_s$ photometry which is available for the whole field in the 2MASS 1999 Spring Incremental Data Release. We describe the determination and analysis of proper motions from photographic plates and recent observations at the meridian circle of Bordeaux (Sect. 2). For 24 bright stars ($V \leq 13$) around the cluster's center, spectra were obtained with the echelle spectrograph ELODIE on the 193cm telescope at the Haute-Provence Observatory. The radial velocities of the red giants were obtained by standard on-line reduction directly at the telescope. The determination of the radial velocity and projected rotational velocity of the hot fast rotating turnoff stars required dedicated reduction tools (Sect. 3). In Sect. 4 we present our analysis of the spectra to estimate the atmospheric parameters $T_{\rm eff}, \log g$, [Fe/H] and the absolute magnitude $M_{\rm V}$. For the latter, we developed a new version of the TGMET method (Katz et al. 1998 and Soubiran et al. 1998). We discuss the case of an unusual giant in NGC 2355 which is 2.3 magnitudes brighter than the giant clump for the same temperature. We also report the discovery of a blue straggler in the cluster and of a moving pair of field stars. Sect. 5 deals with the fundamental parameters of NGC 2355 resulting from our study. Our conclusions are reviewed in Sect. 6. For identifying individual stars we use as far as available the star numbers introduced by Kaluzny & Mazur (1991), preceded by the prefix "KM".

2. Measurement and analysis of proper motions

We determined precise proper motions for stars in the cluster region and in the surrounding field for two reasons: 1. to enable a kinematical segregation of cluster members and non-members, and 2. to derive the absolute tangential velocity of the cluster. In order to achieve adequate accuracy, the proper motions were determined from observations at 3 epochs with a maximum separation of about 90 years. The first epoch, around 1910, was provided by a triple-exposed plate from the Bordeaux Carte du Ciel (CdC, $2^\circ \times 2^\circ$, $B_{\rm lim} \simeq 15.0$) on which the cluster is favorably placed near the plate center, and by 5 plates from the Bordeaux Astrographic Catalogue (AC, same size, $B_{\rm lim} \simeq 12.0$) which fully or partially overlap with the field of the CdC-plate. Second epoch positions were obtained by measurement of two POSS-I glass copies (O & E plates) from the Leiden Observatory plate archive. The third epoch consists of observations made with the CCD meridian circle of Bordeaux Observatory in 1997/1998 as part of the 'Méridien 2000' program (see Colin et al. 1998).

The CdC and POSS plates were scanned on the MAMA machine at the Paris Observatory, the AC plates were scanned on a PDS machine at the Astronomical Institute Münster. The scans were processed partly with the SExtractor software (Bertin & Arnouts 1996) and partly with our own software, in particular for the centering of the CdC triple images. All observations were reduced to the reference system of Hipparcos. The meridian observations and the first-epoch plate measurements were linked directly to reference stars from the Hipparcos catalogue and the ACT Reference catalogue (Urban et al. 1998). Iterative reduction schemes were used in order to make due account of the multiple observations of each star. The measurements from the POSS-I plates required a separate treatment because the geometry of projection on these plates is subject to complicated and sizable distortions. Thus we constructed from the first and third-epoch data an intermediary catalog of secondary reference stars. We then applied a moving-filter technique as described by Morrison et al. (1998) to transform the POSS-I data locally and smoothly to the Hipparcos system. The final proper motions were obtained by combining the positions from all epochs in a weighted linear least-squares adjustment.

According to the reduction residuals and the comparison between different observations of the same epoch, the mean accuracies of the positions are as follows: 50 mas per coordinate for the mean positions from the meridian circle observations, between 120 and 150 mas per coordinate and plate for the positions from the first-epoch plates and 150 mas per coordinate and plate for the positions from POSS-I. The mean internal errors of the resulting proper motions range from $0.7\,{\rm mas\,y^{-1}}$ for the brightest stars to $2.0\,{\rm mas\,y^{-1}}$ for the faintest stars of the sample.

Without selection according to kinematics, the distribution of the stars in the plane of the sky reveals that the cluster is centered on the position $\alpha = 7^{\rm h}17^{\rm m}.0, \delta = 13^\circ 45'$ (2000.0), and that its angular radius is at least $5'$, but probably larger. In Fig. 1 we present histograms of the distribution of proper motions for a circular field of $7'$ radius around the above given position. For comparison we also show the distribution of proper motions in an annulus outside the cluster, namely between $18'$ and $36'$ from the center (counts rescaled to equal surface). It is clearly seen that the cluster stands out against the field as a concentration of comoving stars.

In order to estimate the mean proper motion of the cluster and to obtain cluster membership probabilities we fitted two-dimensional Gaussians to the proper-motion distributions of the pure field sample and the cluster-and-field sample. The parameters of the distributions were determined by applying a maximum-likelihood criterion to the proper motions in the range $\mu_l \cos b \in [-6, +10]\,{\rm mas\,y^{-1}}$ and $\mu_b \in [-10, +6]\,{\rm mas\,y^{-1}}$. The distribution of the field stars appears centered around $(\mu_l \cos b, \mu_b) = (+2.4, -1.8)\,{\rm mas\,y^{-1}}$ and has a dispersion of about $3\,{\rm mas\,y^{-1}}$. The proper motions of the cluster stars are centered on $(\mu_l \cos b, \mu_b) = (+0.5, -2.4)\,{\rm mas\,y^{-1}}$, i.e. they are slightly offset from the mean proper motion of the field, and have a dispersion of $0.8\,{\rm mas\,y^{-1}}$ in $\mu_l \cos b$ and $1.5\,{\rm mas\,y^{-1}}$ in μ_b. The dispersion in μ_b is in agreement

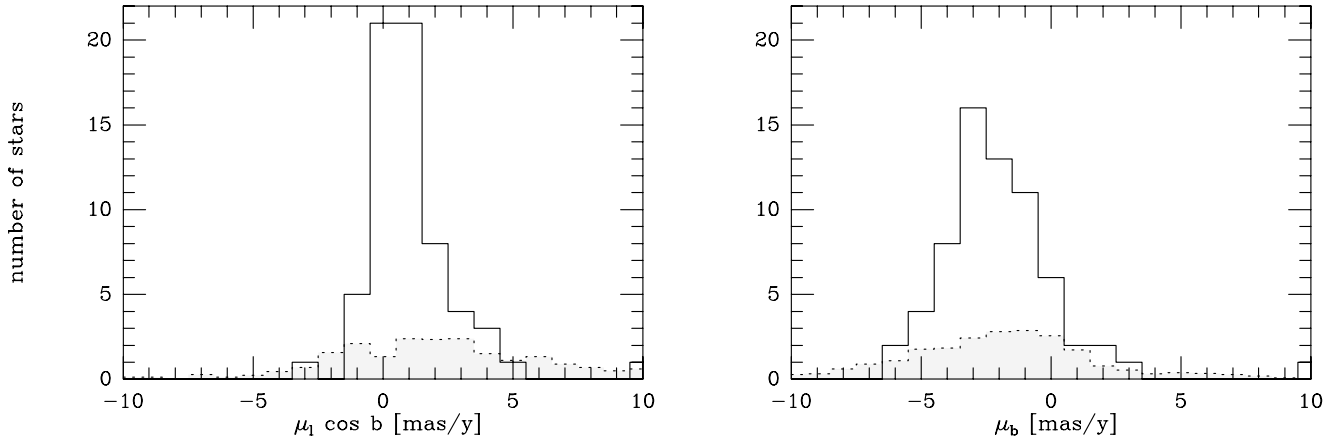

Fig. 1. Distribution of stellar proper motions (in galactic components μ_l, μ_b) in a circular field of $7'$ radius around the center of the cluster (solid line) and in an annulus with radii $18'$ and $36'$ (dotted line). The number counts in the annulus are rescaled to the surface of the circle in order to enable direct comparison.

with the estimated mean proper motion errors. However it is surprising that the dispersion in $\mu_l \cos b$ is substantially smaller. The determination of the mean proper motion of the cluster has a statistical uncertainty of $0.3\,\mathrm{mas\,y^{-1}}$. To this we must add in quadrature the uncertainty of the absolute calibration of the Hipparcos reference frame which is $0.25\,\mathrm{mas\,y^{-1}}$ (Kovalevsky et al. 1997). With some additional allowance for other (possibly undetected) systematic errors in the measuring process we estimate that the accuracy of our determination of the absolute proper motion of the cluster is $0.5\,\mathrm{mas\,y^{-1}}$ per coordinate.

Using the above given parameters for the distributions of the proper motions in the cluster and the field, individual kinematical membership probabilities were calculated. This was done in the usual way according to the relative frequency of cluster stars which the fitted model distributions predict for a given proper motion. Our sample of stars in the $7'$ circle thus divides into 38 probable cluster members ($p > 90\%$), 13 probable field stars ($p < 10\%$) and 17 unclear cases ($10\% \leq p \leq 90\%$).

By kinematical discrimination between cluster stars and field stars one obtains an improved picture of the structure and spatial extent of the cluster. For this purpose we chose a field of $36'$ radius around the cluster center and selected only those stars with proper motion equal to the mean motion of the cluster within 1σ, i.e. the proper motion dispersion of the cluster stars. The latter criterion reduces the surface density of the field stars by a factor of 10, but retains a sufficiently large number of cluster stars so that the cluster's structure and extent become more clearly recognizable. Fig. 2 compares the radial profile of stellar density (number counts in non-overlapping annuli around the cluster center) with and without kinematical selection. It turns out that the cluster has a central component with exponentially decreasing density out to about $7'$, a halo with approximately constant density beyond $7'$ and an edge at $15'$. The core radius of the cluster, i.e. the radius at which the surface density drops to half its central value, is found to be about $1.5'$.

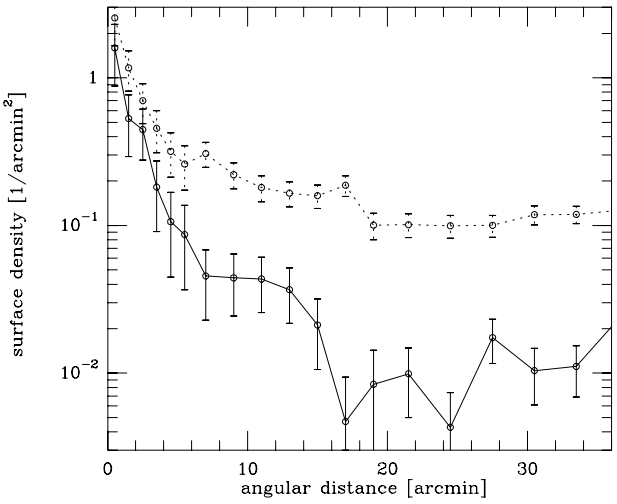

Fig. 2. Radial density profile of the cluster as obtained from star counts down to $B = 15.0$ in non-overlapping annuli around the cluster center. Dotted line: without kinematic selection. Solid line: only stars with proper motion close to the mean motion of the cluster. Error bars show the size of $\sqrt{N}$ variations.

3. Spectroscopy : radial and rotational velocities

Twenty-four stars with $V \leq 13$ in the field of the cluster were observed at the Haute-Provence Observatory in January 1999, on the 1.93m telescope equipped with the spectrograph ELODIE. This instrument is a dual-fibre-fed echelle spectrograph devoted to the measurements of accurate radial velocities (Baranne et al. 1996). A spectral range 390-680 nm is recorded in a single exposure as 67

orders on a 1K CCD at a mean resolving power of 42000. With a one hour exposure one typically achieves a S/N of 100 on a star of magnitude 8.5 or a S/N of 10 on a star of magnitude 12.8. ELODIE is a very stable instrument, allowing to compare easily spectra observed at different epochs.

Optimal extraction and wavelength calibration are automatically performed on-line, as well as the measurement of radial velocities by digital cross-correlation with binary templates thanks to the TACOS reduction software developed by D. Queloz (1996). The cross-correlation technique is well adapted for strong-lined spectra, corresponding to moderate effective temperatures up to 6500 K. The precision of radial velocities for such spectral types is better than $100\,\mathrm{m\,s^{-1}}$ even at low signal to noise ratio. Among the 24 target stars, 16 stars presented a clean deep correlation profile, permitting an accurate radial velocity and FWHM measurement directly at the telescope. The observations revealed a strong concentration of stars at $v_\mathrm{r} \sim 35\,\mathrm{km\,s^{-1}}$. This is without doubt the trace of the radial motion of the cluster. Thus, on the basis of radial velocity, 9 target stars were confirmed to be members of the cluster, with colours corresponding to clump giants. The mean radial velocity of this sub-sample is $35.13\,\mathrm{km\,s^{-1}}$ with a standard deviation of $0.39\,\mathrm{km\,s^{-1}}$. The FWHM of the correlation function was for most of the stars nearly constant at $11.3\,\mathrm{km\,s^{-1}}$, but slightly larger for 3 stars (KM $1 : 13.2\,\mathrm{km\,s^{-1}}$, KM $2 : 34.6\,\mathrm{km\,s^{-1}}$, KM $20 : 17.3\,\mathrm{km\,s^{-1}}$) corresponding to the signature of either macroturbulence, rotation or binarity. The radial velocities are listed in Tab. 1, together with the UBV photometry from Kaluzny & Mazur (1991) and the $\mathrm{JHK_s}$ photometry from 2MASS.

Eight stars with bluer colour presented broad lines indicating a high rotational velocity. They could not be treated by the standard cross-correlation method. Instead, their rotational profile was extracted using a least-squares deconvolution technique developed and fully described by Donati et al. (1997). The latter method presents some similarities with the cross-correlation method. It is based on the fact that the observed spectrum can be expressed as the convolution product of a line pattern with a rotational plus instrumental profile. This profile can thus be recovered by deconvolving the observed spectrum with a line mask computed from a model atmosphere having the same parameters as the star. As the effective temperatures of the target stars were not known, a series of line masks with T_eff ranging from 6000 K to 9000 K were computed from the Kurucz's database (Kurucz 1993). The best contrast was obtained at $T_\mathrm{eff} \sim 7000 - 7500\,\mathrm{K}$. The deconvolution was quite difficult due to the low signal to noise ratio of the spectra but the signature of the rotation was visible for each star and confirmed a radial velocity consistent with the cluster's velocity. The next step was to calibrate the width of the deconvolved profiles in terms of $v \sin i$. For this task we used several reference stars for which both a high-quality ELODIE spectrum and a published value of $v \sin i$ were available. Nine stars from the TGMET library (see next section) were found in the catalogue of rotational velocities compiled by Uesugi & Fukuda (1982), restricted to $50 - 200\,\mathrm{km\,s^{-1}}$. The FWHM of the deconvolved profiles were measured the same way for reference and target stars by fitting a 10 degree polynomial as can be seen in Fig. 3. In this example, the same line mask corresponding to the parameters $T_\mathrm{eff} = 7500K, \log g = 4.0, [\mathrm{Fe/H}] = 0.0$ was used for the deconvolution of the two spectra, but HD 132052 ($v \sin i = 120\,\mathrm{km\,s^{-1}}$) was observed at S/N=131 while KM 13 was observed at S/N=11. The weighted linear regression performed on the 9 points given by the reference stars led to the relation $v \sin i = 0.443 \cdot \mathrm{FWHM} + 19.5\,\mathrm{km\,s^{-1}}$, represented in Fig. 4. The projected rotational velocities estimated for the 8 turnoff stars of NGC 2355 are given in column 10 of Tab. 1.

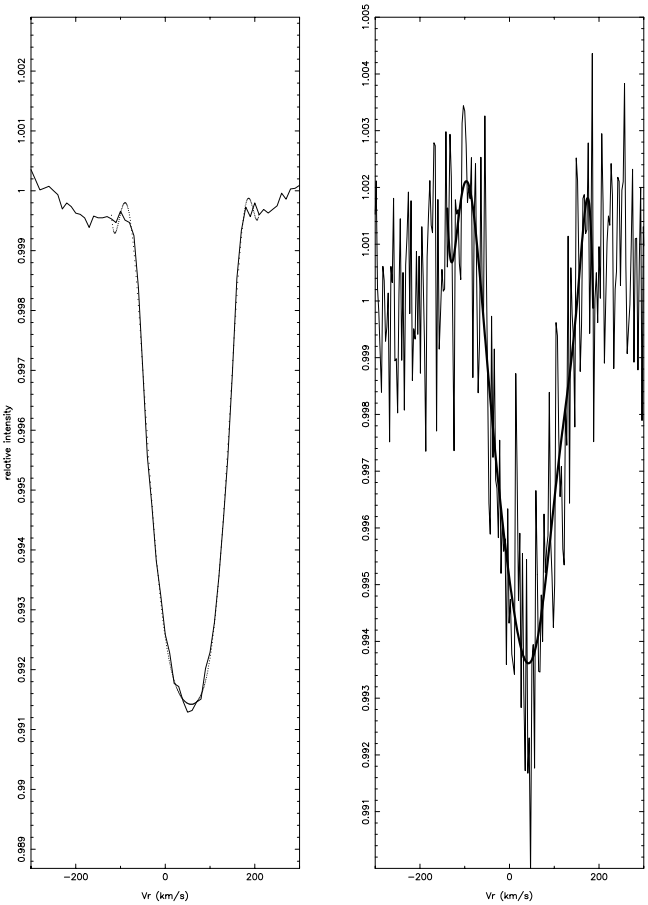

Fig. 3. The deconvolved profiles of HD 132052 (S/N = 131, $v \sin i = 120\,\mathrm{km\,s^{-1}}$) and KM 13 (S/N=11) are fitted with a 10 degree polynomial. The fit on KM 13 gives $v_\mathrm{r} = 40\,\mathrm{km\,s^{-1}}$ (heliocentric), $v \sin i = 90\,\mathrm{km\,s^{-1}}$

The most remarkable star among those which are classified as cluster members in Tab. 1 is KM 1. This is a giant which is 2.3 magnitudes brighter than the giant clump of the cluster. The fact that it is within one sigma of the

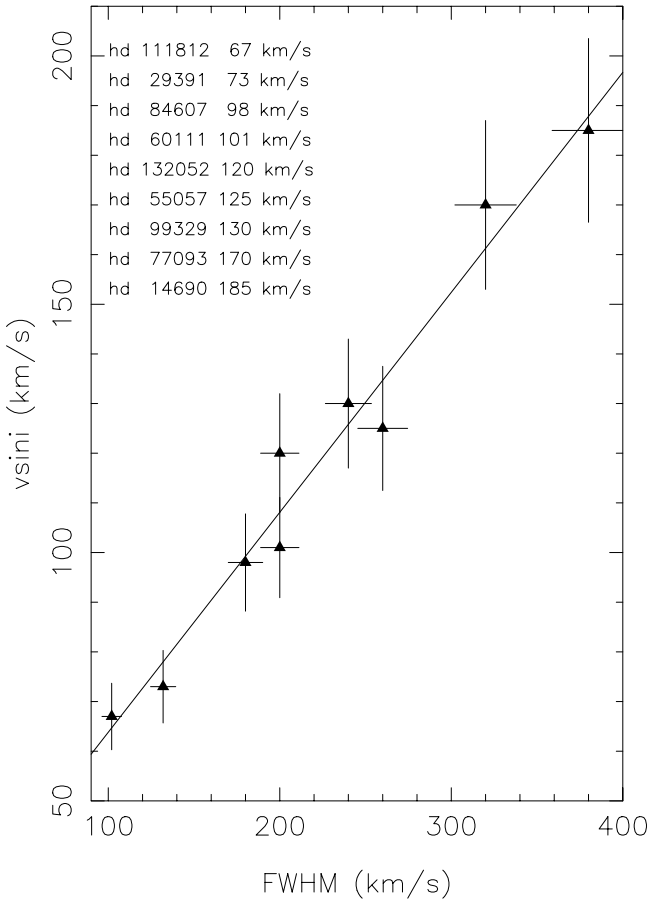

Fig. 4. A linear relation between the measured FWHM of the deconvolved profiles and the projected rotational velocities was computed from 9 reference stars observed also with ELODIE, with known projected rotational velocities from Uesugi & Fukuda (1982). An error of 20% was assumed on the projected rotational velocities taken from the litterature, and the horizontal error bars represent the standard error on the measurement of the FWHM.

cluster distribution in position, proper motion and radial velocity makes us believe that it is a cluster member and not a field star. On the other hand, we cannot completely exclude the possibility that it is a projection of a field star onto the cluster because a field star at this position may by chance have the same radial velocity as the cluster. According to the formulae of the circular motion around the galactic center, a star on the line of sight to the cluster at a distance between 0.5 kpc and 2 kpc would have a heliocentric radial velocity between $+15\,\mathrm{km\,s^{-1}}$ and $+27\,\mathrm{km\,s^{-1}}$. Hence there is a certain overlap between the radial velocity distribution of the field stars and the radial velocity of the cluster.

If KM 1 is a member of the cluster, then it remains unclear by which phenomenon this star is considerably brighter than the other cluster giants of the same colour. We have looked for photometric variations to check if this star could be in an unstable phase of its evolution. No variations could be detected in the meridian observations over 3 years, nor in comparison with the apparent brightness on the 1950 POSS-I plates and the 1910 CdC plate. KM 1 is part of the TYCHO catalogue (TYC 775 997 1) where no variability is reported. The spectrum of this peculiar star is discussed in more detail in the next section.

Another remark is to be made on the star KM 2. This one was selected by Ahumada & Lapasset (1995) as a blue straggler candidate. However, its radial velocity indicates that this star is not a member of the cluster.

We also point towards the stars KM 20 and KM 26. These are found to be field stars with identical radial velocities of $v_\mathrm{r} = 50.3\,\mathrm{km\,s^{-1}}$, despite an angular separation of $1.7'$. The hypothesis of a moving pair is discussed at the end of the next section.

4. Atmospheric parameters, absolute magnitudes

The atmospheric parameters ($T_\mathrm{eff}, \log g, [\mathrm{Fe/H}]$) and the absolute magnitude M_V have been obtained with the automated software TGMET, described in Katz et al. (1998). TGMET is a minimum distance method (reduced χ^2 minimisation) which measures in a quantitative way the similarities and discrepancies between spectra and finds for a given target spectrum the most closely matching template spectra in a library. The TGMET library (Soubiran et al. 1998) was built with high S/N ELODIE spectra of reference stars for which the atmospheric parameters were taken from published detailed analyses, mostly in the Catalogue of [Fe/H] determinations (Cayrel de Strobel et al. 1997). The previous version of the TGMET library was extended to cover the temperature interval [3500 K - 7500 K] and now includes nearly 450 reference spectra of all metallicities. To improve the temperature estimation, the library was also completed with stars having reliable T_eff, either from the list of Blackwell & Lynas-Gray (1998) based on ISO flux calibration, or from the calibration of the colour index V−K (Alonso et al. 1996 and Alonso et al. 1999). A new aspect of TGMET was developed by estimating the absolute magnitude M_V simultaneously with the atmospheric parameters, based on the fact that stars having similar spectra have similar absolute magnitudes. In fact most of the stars of TGMET library are in the Hipparcos catalogue and 313 of them have parallaxes with a relative errors lower than 10%. Stars from the library having precise Hipparcos parallaxes had their absolute magnitude M_V derived from the TYCHO V apparent magnitude. They were used as reference stars for the absolute magnitude as for the atmospheric parameters. Some tests were performed to check the reliability of such spectroscopically determined absolute magnitudes. At solar metallicity, the rms difference between the absolute magnitude determined from Hipparcos and from TGMET is 0.21 for dwarfs, 0.31 for clump giants and 0.50 for other giants. The parameters ($T_\mathrm{eff}, \log g, [\mathrm{Fe/H}], M_\mathrm{V}$) of a target star processed by TGMET are given by the

weighted mean of the parameters of the best matching reference spectra (presenting a reduced χ^2 which does not exceed the lowest one by more than 12%). The resulting uncertainty depends mainly on two factors. The first one is the quality of the parameters found in the literature for the reference stars. Typically errors quoted in detailed analyses are 50 to 150 K for $T_{\rm eff}$, 0.1 to 0.3 for $\log g$, and 0.05 to 0.1 for [Fe/H]. But for some reference stars, it happens that the errors on the atmospheric parameters from the literature are much higher and such stars are gradually being identified with TGMET as outliers. The spectral detailed analysis is the only primary method to estimate metallicities. It is a difficult task and the results obtained by different authors can differ by a large amount. We do not expect to do better than detailed analyses with TGMET, but the method will improve if we can add reference stars with very reliable atmospheric parameters to the library . The problem is not as critical for absolute magnitudes because the large majority of the reference stars have excellent Hipparcos parallaxes thus reliable absolute magnitudes. The second source of uncertainty in the TGMET results is the way the parameter space is sampled by the reference stars. For example, among evolved stars, results are expected to be better for clump giants than for other giants because clump giants are more numerous in the literature and Hipparcos, consequently better represented in the TGMET library than other kinds of giants, and also because clump giants occupy a smaller volume than other giants in the parameter space.

The results of TGMET for the 24 target stars are given in Tab. 2. The last column presents the distance moduli ($V - M_{\rm V}$) of the stars as derived from the spectroscopically determined $M_{\rm V}$. To illustrate the TGMET processing Fig. 5 shows the spectrum of KM 10 in the region of the MgI triplet together with its best matching reference spectrum HD 205435 ($T_{\rm eff} = 5068K, \log g = 2.64, [{\rm Fe/H}] = -0.16, M_{\rm V} = 1.097$). As another example, Fig. 6 represents the H_α line of the fast rotator KM 22 together with its best matching reference spectrum HD 201377 ($M_{\rm V} = 1.607$).

In the previous section, it was pointed out that KM 1 is surprisingly found to be a probable member of the cluster despite a visual magnitude much brighter than the clump giants, for the same colour. Its distance modulus is consistent with the rest of the cluster and hence in agreement with the supposed membership, as well as its metallicity. Nevertheless this star has an abnormal, thus interesting, position on the cluster's HR diagram which is worth attention (see Figs. 7 and 8). The intrinsic physical difference between KM 1 and the other giants of the cluster has been investigated by comparing their respective TGMET best matching reference stars, the parameters of which are presented in Tab. 3. The two sets present similar mean temperatures and metallicities but the range of absolute magnitudes is quite different. KM 1 exhibits through TGMET more spectral similarities with supergiants like HD 215665 or HD 159181 than with clump giants. The larger dispersion which is found for the parameters of KM 1, especially for $M_{\rm V}$, is well explained by the fact that the TGMET library does not sample the parameter space at the same resolution for supergiants than for clump giants as already mentioned. The weighted mean and error bar for each parameter of KM 1 was computed with the 10 best-fitting reference stars, despite large differences, because they equally (within 12%) match the target spectrum. The large error bars reflect the fact that there is not a perfect analog of KM 1 in the TGMET library. Consequently, in the following, KM 1 will contribute with a lower weight than clump giants to the determination of the fundamental parameters of the cluster. The 20 reference stars listed in Tab. 3, except HD 214567, are reported in Uesugi & Fukuda (1982) to rotate at $v \sin i \sim 10-20\,{\rm km\,s^{-1}}$, so that there is no difference between the two sets concerning the rotation. The brighter magnitude of KM 1 could correspond to a higher mass, but in that case KM 1 should be much younger than the other giants. By comparison to the

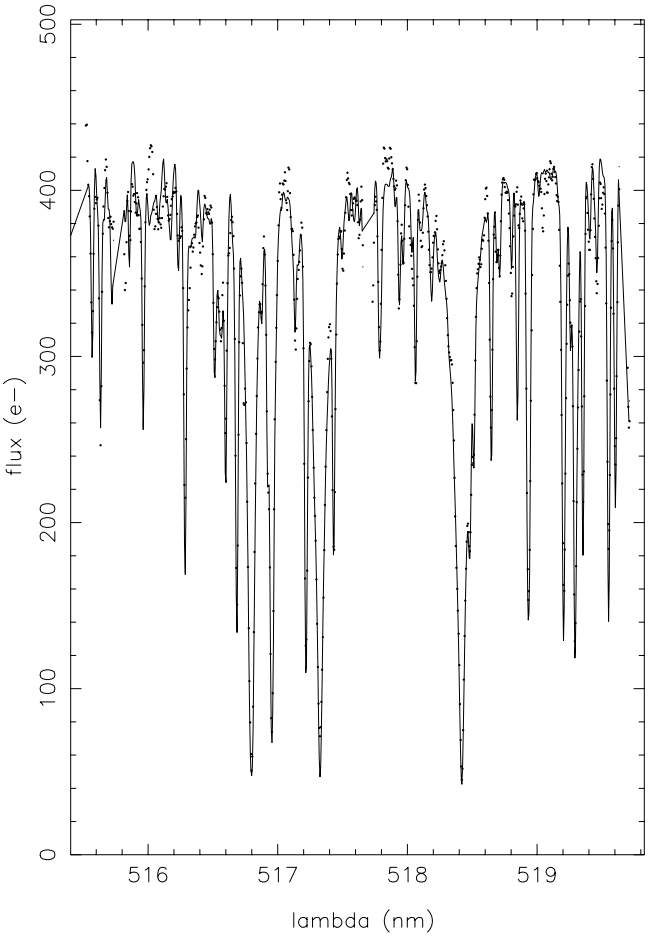

Fig. 5. The spectrum of the clump giant KM 10 (dots) in the region of the MgI triplet together with the best matching reference spectrum, HD 205435 (S/N=164). The reference spectrum was put at the same radial velocity scale and flux level as the target.

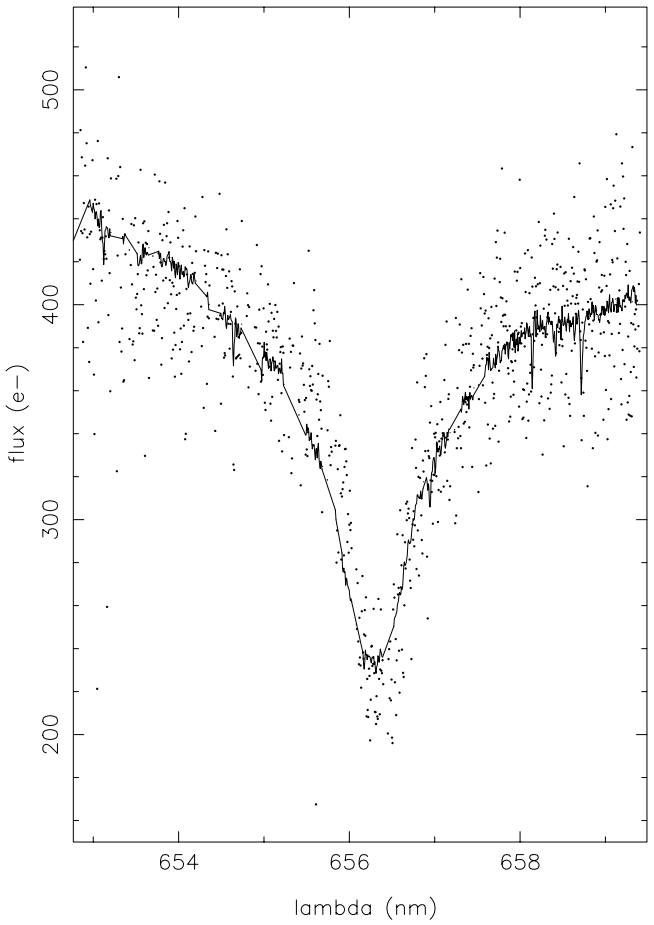

Fig. 6. Same as Fig. 5 for the fast rotator KM 22 and HD 201377 (S/N=167) in the region of H_α.

Table 3. Mean parameters from the literature and Hipparcos of the reference spectra matching the best the target spectra of KM 1 and clump giants of NGC 2355. The parameters of KM 1 were computed from the weighted mean of these 10 reference stars which equally (within 12%) fit the KM 1 spectrum. The 10 reference stars which are presented for cluster's clump giants correspond to those which occur the most often in the TGMET solution of KM 3, KM 4, KM 8, KM 9, KM 10, KM 15, GSC 500538 and GSC 501198.

name	$T_{\rm eff}$	$\log g$	[Fe/H]	$M_{\rm V}$
		KM 1		
HD 203387	4959	2.74	−0.05	0.183
HD 210807	4949	2.52	−0.19	−0.527
HD 215665	4835	2.47	−0.09	−1.470
HD 198809	5087	2.88	−0.14	0.461
HD 185758	5303	2.91	−0.15	−1.433
HD 159181	5169	1.54	0.16	−2.425
HD 206859	4604	1.56	0.00	−2.881
HD 26630	5183	1.40	−0.03	−2.577
HD 209750	5156	1.34	0.17	−3.889
HD 3712	4611	2.04	−0.10	−2.003
		clump giants		
HD 198809	5087	2.88	−0.14	0.461
HD 27022	5100	2.47	0.05	0.241
HD 214567	4994	2.70	0.03	0.481
HD 188119	4885	2.61	−0.32	0.592
HD 205435	4950	2.64	−0.16	1.097
HD 5395	4770	2.55	−0.70	0.628
HD 135722	4810	2.56	−0.44	0.718
HD 210807	4949	2.52	−0.19	−0.527
HD 222404	4778	2.98	−0.01	2.510
HD 35369	4873	2.50	−0.26	0.489

isochrones of Girardi et al. (2000) in the plane $(T_{\rm eff}, M_{\rm V})$, KM 1 should be 160 Myr old whereas the rest of the cluster is 1 Gyr old (see next section). This phenomenon is similar to the blue stragglers phenomenon, but on the red, evolved side. Ahumada & Lepasset (1995) enumerate several theories which have been proposed for the blue stragglers, and which could also explain the observation of KM 1: a field star captured by the cluster, a star which has accreted mass from the interstellar medium, a star which formed after the bulk of the cluster members, the result of a non-standard mechanism in the evolution, the result of a stellar collision or a binary merger. KM 1 could also be a blue straggler which has evolved. At the present state, the main difference observed between the spectra of KM 1 and the clump giants is a slightly broadened profile as seen on macroturbulent supergiants, or on rotating or binary giants, and a difference in absolute magnitude detected by TGMET. A spectrum with much higher S/N is necessary in order to obtain further insight on the nature of this star.

Also mentioned in the previous section, KM 20 and KM 26 might be a moving pair because they have a common radial velocity of $50.3\,{\rm km\,s^{-1}}$. Their metallicities of −0.26 and −0.31 are in agreement. Unfortunately, the other parameters determined for KM 20 present large standard errors (see Tab. 2) indicating that the fit with the TGMET reference spectra was not satisfactory. We recall that KM 20 has an enlarged profile with FWHM = $17.3\,{\rm km\,s^{-1}}$. Thus this star might be a spectroscopic binary which would explain the mediocre results of TGMET. Since a precise estimate of the proper motion of KM 26 is missing (no measurement due to the blending of the image by a reseau line of the CdC plate) the common motion cannot be assessed by means of proper motions. Anyway, the proper motion of KM 20 is small ($\mu_l \cos b = -2.2\,{\rm mas\,y^{-1}}, \mu_b = -1.6\,{\rm mas\,y^{-1}}$), so a large distance is probable and the verification of common proper motion would be difficult. Based on the spectroscopic estimate of the distance of KM 26 (2.7 kpc), the angular separation corresponds to a linear distance between the two stars of 1.3 pc.

5. Fundamental parameters of the cluster

5.1. Metallicity, age, reddening, distance, size

The weighted average of [Fe/H] of the members of NGC 2355 listed in Tab. 2 gives a metallicity of [Fe/H] = -0.07 ± 0.11. The standard error on [Fe/H] does not take into account the uncertainties on [Fe/H] for the reference stars which are usually unknown. For example, the reference clump giant HD 5395 (see Tab. 3), with [Fe/H] = -0.70, has been used to derive the parameters of KM 3, KM 4 and GSC 500538, despite an uncertain metallicity : Fernandes-Villacanas et al. (1990) report [Fe/H] = -1.0, McWilliam (1990) [Fe/H] = -0.51 whereas TGMET gives a value of [Fe/H] = -0.44. This illustrates the difficulty to define a precise reference system for the atmospheric parameters. In this light, the error bar on [Fe/H] is underestimated. We have estimated the age of NGC 2355 by chosing in the isochrones of solar abundance of Girardi et al. (2000) the one which matched the best our observations in the plane ($T_{\rm eff}, M_{\rm V}$). Fig. 9 shows that an age of 1 Gyr is probable due to the position of the turnoff stars.

Despite an unexpectedly dispersed photometry, as previously mentioned by Kaluzny & Mazur (1991), Ann et al. (1999) and confirmed with JHK$_s$, which can be interpreted as the consequence of an inhomogeneous interstellar absorption, the UBV and JHK$_s$ photometry gives an opportunity to estimate the reddening of the cluster and to test at the same time our temperature scale. By inverting the empirical relations $T_{\rm eff} = f(\text{colour}, [\text{Fe/H}])$ calibrated by Alonso et al. (1996) for dwarfs and by Alonso et al. (1999) for giants, the colour index B−V and V−K corresponding to the TGMET effective temperatures were computed and compared to the observed ones, adopting K$_s$ for K. A systematic difference between them can be interpreted either in terms of reddening or as an error in the temperature scale. Giants have been tested first because their TGMET temperature scale is more reliable than for fast rotators. The mean observed colours B−V and V−K for the cluster's giants are respectively 1.04 and 2.54, for a mean effective temperature of 5000 K. Such a temperature at [Fe/H] = -0.07 corresponds to B−V=0.88 and V−K=2.12 in the Alonso et al.'s temperature scale. The corresponding excesses $E_{B-V} = 0.16$ and $E_{V-K} = 0.42$ lead to a ratio $E_{V-K}/E_{B-V} = 2.62$ which agrees, within the error bars, with the value of 2.7 reported by Rieke & Lebofsky (1985) and Cardelli et al. (1989) for the interstellar extinction. For the hot stars the ratio was slightly different, possibly indicating an error in the temperature scale. The mean observed V−K of the dwarfs (1.00), corrected by $E_{V-K} = 0.42$ leads to $T_{\rm eff}$=7500 K with Alonso et al.'s relations while the mean temperature estimated by TGMET is 7300 K. An offset of 200 K in $T_{\rm eff}$ is still consistent with an age of 1 Gyr.

The individual distance moduli of the cluster members in Tab. 2 yield a mean distance modulus of 11.56 ± 0.10 for the cluster. By correcting for interstellar absorption according to a mean reddening of $E_{B-V} = 0.16$ and $A_{\rm V}/E_{B-V} = 3.09$ (Rieke & Lebofsky 1985), we determine the distance of NGC 2355 as 1650^{+80}_{-70} pc. The corresponding height above the galactic plane is 340 pc. The dereddened distance modulus $(V - M_{\rm V})_0 = 11.06$ is consistent with the one derived by Ann et al. (1999), $(m - M)_0 = 11.4$, by isochrone and ZAMS fittings on colour-magnitude diagrams whereas they find a lower metallicity ([Fe/H] = -0.32) and a higher reddening ($E_{B-V} = 0.25$). On the contrary, we are in disagreement with Kaluzny & Mazur (1991) for the distance modulus ($(m-M)_0 = 12.1$) but in better agreement for the metallicity and reddening ([Fe/H] = $+0.13, E_{B-V} = 0.12$). Isochrone and ZAMS fitting is well adapted for dense clusters with high quality multicolour photometry because of the three parameters to be deduced simultaneously : age, metallicity and reddening. In the case of NGC 2355, where the photometry is dispersed, this method can lead to a wide range of parameters as can be seen from the compared studies of Ann et al. (1999) and Kaluzny & Mazur (1991). Spectroscopy concerns less stars but better constrains the parameters. In Sect. 2, the angular radius of the cluster's central body was estimated to be $7'$, while that of its halo was estimated to be $15'$. At the distance of 1.65 kpc this corresponds to linear radii of 3.3 pc and 7.2 pc respectively. The radius of the central body, 3.3 pc, is typical of the old open clusters linear radii which are distributed in a small range with a median at 2.65 pc, and an upper quartile at 3.45 pc (Janes & Phelps 1994).

Fig. 8 presents the dereddened colour magnitude diagram of the cluster in (V−K,V), including the members which have been confirmed by their radial velocity, and the candidates within $7'$ of the cluster's center having a probability higher than 90% to be member on the basis of proper motion. For comparison the 1 Gyr isochrone has been transformed into observable quantities and overlayed. The bluest star, GSC 501264, in the prolongation of the main sequence, is a typical blue straggler candidate. According to its colour $(J - K)_0 = 0.03$, Alonso et al.'s calibration gives an effective temperature of 8300 K. The colour index $(J-H) = 0.09$, for which the reddening is unknown, gives a consistent temperature but $(V - K)_0 = 0.19$ is unfortunately outside the limits of the calibration. It was not possible to estimate spectroscopically such a high temperature with TGMET because of the limit of the library to 7500 K. The effective temperature of blue stragglers seems to correspond to a mass which is higher than that of the turnoff stars, consequently unconsistent with the age of the cluster. This phenomenon was already mentioned in the case of the red giant KM 1 in Sect. 4.

5.2. Space velocity and galactic orbit

Combining our results for the absolute proper motion, radial velocity and distance of the cluster, we determine

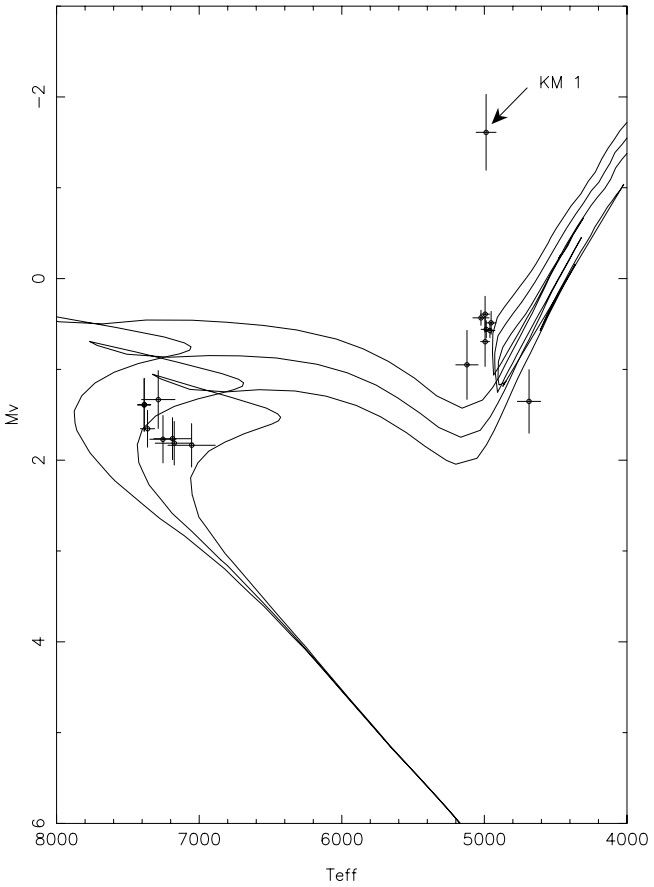

Fig. 7. HR diagram of NGC 2355 from the TGMET parameters. Superposed are the solar metallicity isochrones of Girardi et al. (2000) corresponding to log(age yr)= 8.9, 9.0, 9.1.

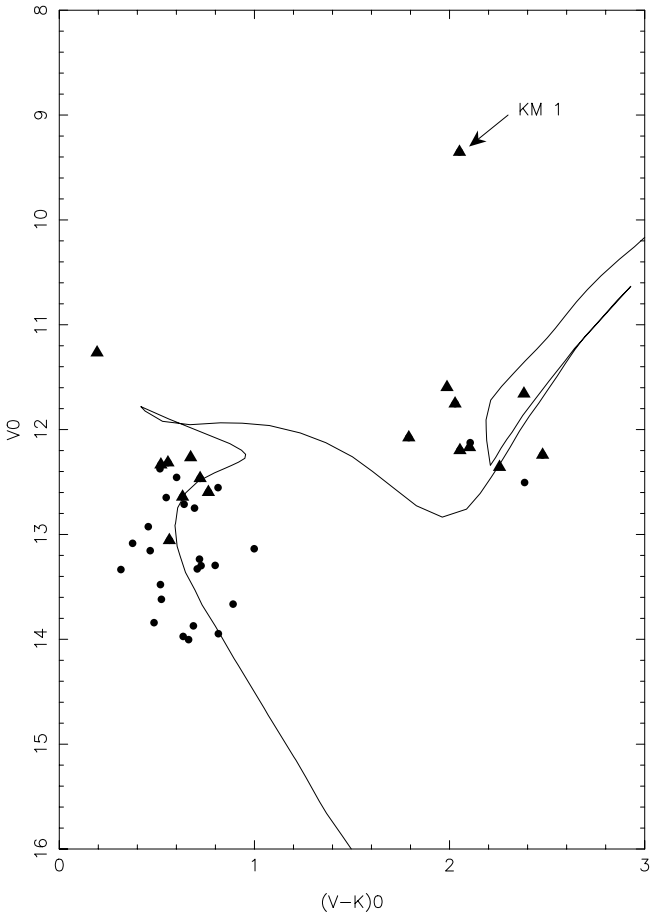

Fig. 8. Dereddened colour-magnitude diagram of NGC 2355. Triangles correspond to radial velocity members, circles to proper motion members. The solid line corresponds to the solar metallicity 1 Gyr isochrone of Girardi et al. (2000).

its heliocentric space motion as $(U, V, W) = (-33.5 \pm 1.8, -18.8 \pm 3.6, -11.2 \pm 3.9)\,\mathrm{km\,s^{-1}}$ [1]. The uncertainties in the components of the space motion result from the combination of all estimated observational errors which were given in the previous sections. However, due to the relatively large distance of the cluster from the Sun, the error budget is dominated by the uncertainty in the cluster's proper motion.

In order to obtain the velocity of the cluster in the galactocentric frame, we assume the motion of the Sun in the LSR as $(U, V, W)_\odot = (9.7, 5.2, 6.7)\,\mathrm{km\,s^{-1}}$, following the recent result of Bienaymé (1999) which is supported by similar results of e.g. Dehnen & Binney (1998). Furthermore we adopt the current IAU standard values of $V_{LSR} = 220\,\mathrm{km\,s^{-1}}$ for the local circular rotation velocity and $R_\odot = 8.5$ kpc for the distance of the Sun from the galactic center. The galactocentric position and velocity of the cluster then is $(x, y, z) = (-10.00, -0.64, +0.34)$ kpc and $(U, V, W) = (-23.5, +206.2, -4.2)\,\mathrm{km\,s^{-1}}$. Together with the galactic gravitational potential these vectors determine the orbit of the cluster in the Galaxy.

We have integrated the equations of motion in the galactic model of Allen & Santillan (1991) over the estimated cluster age of 1 Gyr. The resulting orbit is characterized by radial oscillations between distances from the galactic center of 8.9 and 10.1 kpc and vertical oscillations with an amplitude of 350 pc. The median of the distance r from the galactic center along the orbit is 9.6 kpc and the median of the distance $|z|$ from the galactic plane is 0.24 kpc. The cluster has made 3.7 revolutions around the galactic center and 21 crossings of the galactic disk within its lifetime. If one varies the measured space velocity of the cluster within the error bars of the observations the parameters of the orbit undergo relatively small changes. We find that the radial distances can differ by ±3% and the vertical distances by ±7% from the above given values for the 'mean orbit'. Thus we can say with certainty that the cluster keeps well outside the solar circle throughout its revolution around the Galaxy.

[1] To be clear, U,V,W are vector components with respect to a right-handed triad pointing to galactic center, direction of rotation and northern galactic pole

We currently observe the cluster close to its maximum distance from the plane, i.e. close to the point of reversal of the vertical oscillation. This is consistent with the characteristics of the vertical motion because the probability to find the cluster near the maximum of $|z|$ (at a randomly chosen instant) is about a factor of three larger than the corresponding probability for a lower value of $|z|$. The statistics of $|z|$ along the orbit is such that the cluster spends only 9% of its time in the thin layer of the young disk population at $|z| \leq 50$ pc where close encounters with very massive molecular clouds could have occurred. On the other hand, the orbit of NGC 2355 does not reach such extreme vertical distances as a few other old open clusters which are found at $|z|$ up to 2.4 kpc (Friel 1995). Thus we recognize NGC 2355 as a fairly normal representative of the old open cluster population. The latter has a scale height of 375 pc (Janes & Phelps 1994) as compared to the scale height of 55 pc for the young population of open clusters.

6. Conclusion

We have presented a detailed study of stars in the region of NGC 2355, combining new astrometric and spectroscopic data with recent photometric data from other sources. Our main results can be summarised as follows :

- NGC 2355 is at 1.65 kpc of the Sun and 340 pc above the galactic plane in the direction of the anticenter, with a reddening of $E_{B-V} = 0.16$ and $E_{V-K} = 0.42$.

- Its metallicity is [Fe/H] $= -0.07 \pm 0.11$ and its age is 1 Gyr.

- NGC 2355 has a core radius of about 0.7 pc, a central component with a radius of 3.3 pc and a halo out to 7.2 pc from the cluster center.

- The turnoff stars of NGC 2355 are fast rotators, with a mean projected rotational velocity of $100\,\mathrm{km\,s^{-1}}$ and a mean $T_{\rm eff}$ of 7500 K.

- The giant clump is well defined at $T_{\rm eff} = 5000K$, $M_{\rm V} = 0.51$.

- Two stragglers have been identified in the cluster: a blue one, and a giant which has an unusual position in the HR diagram, 2.3 mag brighter than the giant clump.

- NGC 2355 has a galactocentric space velocity vector $(U, V, W) = (-23.5, +206.2, -4.2)\,\mathrm{km\,s^{-1}}$ and an orbit which keeps it beyond the solar circle and with only brief passages through the galactic plane.

As a by-product of the study of the cluster, we found a moving pair of field giants with a radial velocity of $50\,\mathrm{km\,s^{-1}}$.

Acknowledgements. We thank J.Guibert and the MAMA team at Paris Observatory for their support by scanning plates, R. LePoole from Leiden Observatory for lending the POSS-I glass copies, the Astronomical Institute Münster for scanning time on the PDS machine, and all colleagues of Bordeaux Observatory who have taken part in the meridian circle observations. We also thank C. Catala who provided his observations to increase the TGMET library, J.-F. Donati who kindly made his deconvolution software available for us, J.-L. Halbwachs and S. Piquard who provided some intermediate measurements of TYCHO, and A. Alonso who provided his calibrations before publication. We are also grateful to R. Cayrel for his comments and suggestions. We have made use in this research of the SIMBAD and VIZIER databases, operated at CDS, Strasbourg, France. M.O. gratefully acknowledges financial support by a Marie Curie research grant from the European Community during this work.

References

Ahumada J., Lapasset E., 1995, A&AS 109, 375.
Allen C., Santillan A., 1991, Rev. Mex. Astron. Astrofis. 22, 255.
Alonso A., Arribas S., Martínez-Roger C., 1996, A&A 313, 873.
Alonso A., Arribas S., Martínez-Roger C., 1999, A&AS 140, 261.
Ann H.B., Lee M.G., Chun M.Y., Kim S.-L., Jeon Y.-B., Park B.-G., Yuk I.-S., Sung H., Lee S.H., 1999, JKAS 32, 7.
Baranne A., Queloz D., Mayor M., Adrianzyk G., Knispel G., Kohler D., Lacroix D., Meunier J.-P., 1996, A&AS 119, 373.
Bertin E., Arnouts S., 1996, A&AS 117, 393.
Bienaymé O., 1999, A&A 341, 86.
Blackwell D.E., Lynas-Gray A.E., 1998, A&AS 129, 505.
Cardelli J.A., Clayton G.C., Mathis J.S., 1989, ApJ 345, 245.
Cayrel de Strobel G., Soubiran C., Friel E.D., Ralite N., François P., 1997, A&AS 124,299.
Colin J., Daigne G., Ducourant C. et al., 1998, in: Brosche P, Dick W.R., Schwarz O., Wielen R. (eds.), The Message of the Angles - Astrometry from 1798 to 1998, Acta Historica Astronomiae Vol. 3, Harri Deutsch, Frankfurt, p.133
Dehnen W., Binney J.J., 1998, MNRAS 298, 387.
Donati J.-F., Semel M., Carter B.D., Rees D.E., Cameron A.C., 1997, MNRAS 291, 658.
Fernandes-Villacanas J.L., Rego M., Cornide M., 1990, AJ 99, 1961.
Friel E.D., 1995, ARAA 33, 381.
Girardi L., Bressan A., Bertelli G., Chiosi C., 2000, A&AS 141, 371.
Janes K. A., Phelps R. L., 1994, AJ 108, 1773.
Kaluzny J., Mazur B., 1991, AcA 41, 279.
Katz D., Soubiran C., Cayrel R., Adda M., Cautain R., 1998, A&A 338, 151.
Kovalevsky J., Lindegren L., Perryman M., et al., 1997, A&A 323, 620.
Kurucz R.L., 1993, CD-ROM 13.
McWilliam A., 1990, ApJS 74, 1075.
Morrison J., Smart R.L., Taff L.G., 1998, MNRAS 296, 66.
Queloz D., 1996, ELODIE user's guide, http://www.obs-hp.fr/
Phelps R. L., Janes K. A., Montgomery K. A., 1994, AJ 107, 1079.
Rieke G.H., Lebofsky M.J., 1985, ApJ 288, 618.
Soubiran C., Katz D., Cayrel R., 1998, A&AS 133, 221.
Uesugi A., Fukuda I., 1982, Department of Astronomy, Kyoto University, Japan. Available at the CDS.
Urban S.E., Corbin T.E., Wycoff G.L., 1998, AJ 115, 2161.

Table 1. List of the 24 stars in the field of NGC 2355 observed with ELODIE. UBV photometry is from Kaluzny & Mazur (1991)(*: CCD meridian V photometry), JHK$_s$ is from 2MASS. S/N is the mean signal to noise ratio of the spectrum at 550 nm. v_r (heliocentric) results from the standard on-line reduction and $v \sin i$ from the least-square deconvolution method (see text).

object	V	B−V	U−B	J	H−K$_s$	J−K$_s$	S/N	v_r	$v \sin i$	member
KM 1	9.847	1.059	0.834	7.952	0.135	0.576	16	35.57	-	yes
KM 2	11.896	0.367	0.102	11.077	0.012	0.177	12	10.22	-	no
KM 3	12.152	0.950	0.828	9.845	0.115	0.494	16	34.79	-	yes
KM 4	12.247	1.004	0.729	10.360	0.172	0.561	14	34.89	-	yes
KM 6	12.612	1.146	1.050	10.537	0.129	0.673	9.5	61.22	-	no
KM 7	12.619	1.011	0.681	10.705	0.096	0.612	11	19.98	-	no
KM 8	12.663	1.027	0.762	10.738	0.142	0.597	9	35.73	-	yes
KM 9	12.692	1.025	0.759	10.769	0.060	0.550	14	35.06	-	yes
KM 10	12.736	1.176	0.965	10.504	0.167	0.665	19	35.03	-	yes
KM 11	12.755	1.064	0.749	10.734	0.152	0.622	14	−32.43	-	no
KM 12	12.760	0.396	0.242	11.844	0.100	0.177	5.5	-	90	yes
KM 13	12.809	0.341	0.210	12.033	0.033	0.201	11	-	90	yes
KM 14	12.829	0.330	0.193	12.032	0.034	0.144	7	-	120	yes
KM 15	12.852	1.128	1.095	10.838	0.115	0.662	17	34.72	-	yes
KM 19	12.958	0.412	0.255	12.013	0.071	0.197	18	-	120	yes
KM 20	12.999	1.164	0.841	10.800	0.138	0.605	13	50.29	-	no
KM 21	13.091	0.432	0.206	12.138	0.019	0.231	8	-	105	yes
KM 22	13.136	0.394	0.243	12.240	−0.017	0.156	15	-	125	yes
KM 26	13.466	1.100	0.812	11.382	0.209	0.636	14	50.31	-	no
KM 27	13.550	0.394	0.273	12.713	0.010	0.147	13	-	105	yes
GSC 77500538	12.09*	-	-	10.280	0.149	0.597	7	35.68	-	yes
GSC 77501060	12.09*	-	-	9.669	0.155	0.798	21	−42.62	-	no
GSC 77501198	12.57*	-	-	10.865	0.096	0.506	12	34.70	-	yes
GSC 77501264	11.76*	-	-	11.259	0.019	0.113	9	-	115	yes

Table 2. Atmospheric parameters ($T_{\rm eff}, \log g, [{\rm Fe/H}]$) and absolute magnitude $M_{\rm V}$ obtained with TGMET, and standard errors. Column 7 indicates the reference star which was found to have the most similar spectral characteristics over the considered wavelength interval. The last column gives the distance modulus ($V - M_{\rm V}$).

object	member	$T_{\rm eff}$	$\log g$	[Fe/H]	$M_{\rm V}$	best reference	$V - M_{\rm V}$
KM 1	yes	4988 ± 70	2.16 ± 0.19	-0.04 ± 0.04	-1.611 ± 0.417	HD 203387	11.451
KM 2	no	6835 ± 54	–	-0.28 ± 0.04	2.768 ± 0.215	HD 18995	9.122
KM 3	yes	4987 ± 36	2.72 ± 0.07	-0.14 ± 0.06	0.559 ± 0.096	HD 27022	11.591
KM 4	yes	4961 ± 35	2.67 ± 0.06	-0.15 ± 0.08	0.572 ± 0.079	HD 5395	11.668
KM 6	no	4835 ± 60	2.84 ± 0.12	-0.17 ± 0.04	1.138 ± 0.288	HD 185351	11.472
KM 7	no	4898 ± 40	2.65 ± 0.07	-0.50 ± 0.08	0.998 ± 0.222	HD 127243	11.612
KM 8	yes	5122 ± 78	2.75 ± 0.10	-0.23 ± 0.06	0.950 ± 0.380	HD 198809	11.710
KM 9	yes	4995 ± 32	2.64 ± 0.05	-0.12 ± 0.05	0.392 ± 0.197	HD 198809	12.298
KM 10	yes	4995 ± 31	2.76 ± 0.08	-0.15 ± 0.05	0.694 ± 0.274	HD 205435	12.036
KM 11	no	4893 ± 50	2.65 ± 0.06	-0.50 ± 0.06	1.193 ± 0.199	HD 219615	11.557
KM 12	yes	7254 ± 92	4.30 ± 0.20	0.02 ± 0.02	1.769 ± 0.261	HD 99329	10.991
KM 13	yes	7187 ± 131	4.30 ± 0.20	-0.08 ± 0.10	1.763 ± 0.231	HD 193581	11.037
KM 14	yes	7175 ± 133	4.14 ± 0.20	-0.11 ± 0.08	1.813 ± 0.240	HD 169032	11.007
KM 15	yes	4687 ± 82	2.77 ± 0.11	0.00 ± 0.03	1.353 ± 0.350	HD 222404	11.497
KM 19	yes	7386 ± 45	–	–	1.394 ± 0.291	HD 169032	11.556
KM 20	no	5126 ± 120	3.02 ± 0.20	-0.26 ± 0.09	1.793 ± 0.438	HD 27022	11.197
KM 21	yes	7053 ± 166	–	-0.28 ± 0.25	1.836 ± 0.239	HD 99329	11.254
KM 22	yes	7385 ± 46	–	–	1.387 ± 0.289	HD 169032	11.743
KM 26	no	4908 ± 41	2.68 ± 0.08	-0.31 ± 0.06	0.843 ± 0.267	HD 188119	12.617
KM 27	yes	7362 ± 50	–	0.06 ± 0.06	1.654 ± 0.203	HD 193581	11.896
GSC 500538	yes	4953 ± 36	2.66 ± 0.06	-0.22 ± 0.07	0.488 ± 0.126	HD 27022	11.602
GSC 501060	no	4359 ± 62	2.02 ± 0.13	-0.17 ± 0.04	-0.143 ± 0.472	HD 5234	12.233
GSC 501198	yes	5024 ± 57	2.66 ± 0.10	-0.14 ± 0.09	0.432 ± 0.083	HD 198809	12.138
GSC 501264	yes	7287 ± 117	4.30 ± 0.20	0.03 ± 0.03	1.332 ± 0.319	HD 201377	10.428

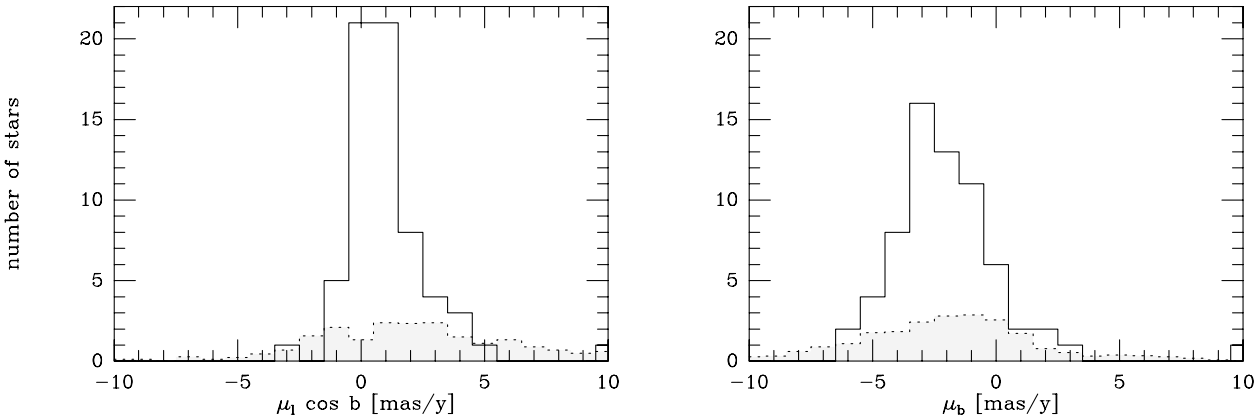
number of stars
20
15
10
5
0
−10
−5
0
5
10
μ_l cos b [mas/y]
20
15
10
5
0
−10
−5
0
5
10
μ_b [mas/y]

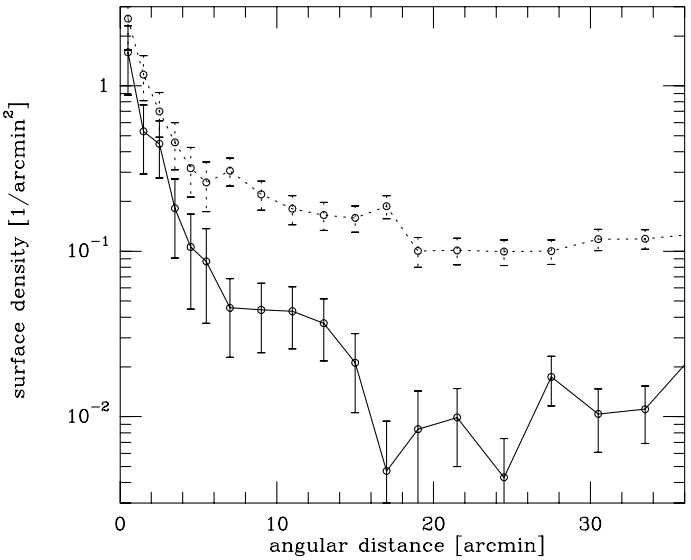
surface density [1/arcmin^2]
1
10^{-1}
10^{-2}
0
10
20
30
angular distance [arcmin]